Effects of Spanwise Flexibility on Lift and Rolling Moment of a Wingsail

EFFECTS OF SPANWISE FLEXIBILITY ON LIFT AND ROLLING MOMENT OF A WINGSAIL

Sheila Widnall
Department of Aeronautics and Astronautics
Massachusetts Institute of Technology

Hayden Cornwell
Department of Aeronautics and Astronautics
Massachusetts Institute of Technology

Peter Williams
Department of Aeronautics and Astronautics
Massachusetts Institute of Technology

Abstract: An aerodynamic theory is developed to determine the lift and rolling moment on a wingsail with a spanwise-flexible flap. The flap is attached to a forward rigid wing by means of a torsion bar, which allows the flap to deflect under the aerodynamic moment acting on the flap. The torsion of the bar is chosen to obtain the desired reduction in rolling moment as a function of wind speed. The lift and rolling moment of the wing sail is compared to that for a rigid wingsail as a function of wind speed. The results show that the rolling moment of a wingsail with a flexible flap can be significantly reduced in an adaptive manner at increasing wind speeds as compared to that of a rigid wingsail. Calculations are performed for a wing of constant chord, a wing of linearly varying chord, and for torsion rods of constant and spanwise varying stiffness. A non-dimensional parameter is identified allowing a wingsail designer to identify the required torsional stiffness for a wing of arbitrary span at a desired wind speed.

Keywords: aerodynamics, performance predictions, sails

NOMENCLATURE

α	Wing angle of attack
α_1	Flap angle of attack
c(y)	Chord
C_L	Lift coefficient
C_m	Rolling moment coefficient
κ	Torsional stiffness
m	Rolling moment
M	Torsional moment
U	Wind speed
Y	Wing span

INTRODUCTION

Several authors have considered the optimization of spanwise loading on a wing, subject to different constraints. Jones (1950) calculated the optimum spanwise lift distribution for a wing subject to a constraint on lift and root bending moment. Wood and Tan(1978) applied these ideas to determine the optimum spanwise lift distribution for a yacht sail subject to a constraint on the rolling moment while maximizing forward thrust. Subsequent authors, such as Junge et.al. (2010) and Sneyd and Sugimoto (1997) extended the analysis to include spanwise variation of wind strength and direction and boat heel. All of these analyses confirm the importance of maximizing lift and/or forward thrust while constraining rolling moment. In the analysis of a yacht, the geometry of the wind direction relative to the yacht direction is such that aerodynamic lift on the wing provides a component of forward thrust on the yacht. Thus we will occasionally use the terms lift and thrust interchangeably.

These previous analyses focused on the design of a wing or a fixed sail planform optimized to operate at a given wind speed. As sailing has moved to the use of wingsails, the analysis of the sail overlaps with traditional aerodynamics. However, unlike an aircraft wing which is designed to operate at a given flight speed, and is equipped with devices such as flaps for lower landing speeds, a racing yacht operates over a wide range of wind speeds. Typical values would range from 10-30 kts, at which point the race would be called off.

This paper investigates the use of spanwise deformable wings to allow the wingsail to operate in a naturally occurring adaptive manner over a wider range of wind speeds while still constraining rolling moment. The current research done in spanwise-deformable wings focuses on the flapping motion of "bio-inspired" wings, Harmon (2009). It is observed in birds and insects that their wings have a significant deformation in the span-wise direction on the downward and upward motions. Researchers are trying to capture a common trend in natural flapping wing motions to apply to future autonomous ornithopter (flapping) designs. Flapping motion is not directly relevant to our study, however we can use some of this research to help predict the behavior of a deformable wingsail. The motion tracking technology used in these experiments indicates that the airfoil deforms at a greater angle at the tip of the wing than at the root.

Large catamarans, as are used in the America's Cup, have large wingsails with a high aspect ratio. These wings are very effective and can generate significant thrust. However, these wingsails are not always trimmed to give optimum performance, and due to the large span of the wing can create extreme rolling moments. For soft sails, the sail can be trimmed in order to depower the sail, and can be reefed -reducing the span- at high wind velocities. In the wingsail case, the rolling moment can be reduced by having multiple vertical sections that can be individually controlled by the crew to give a desired spanwise twist, as described in Fisher (2013). Altering these sections already leads to a decrease in performance, but the fact that these are manually controlled by the crew means that the sail is not trimmed at its optimized potential. Also, given that the crew has other responsibilities, there are more chances for the boat to capsize in an emergency. When boats capsize, especially boats used in the America's Cup, it is highly dangerous for the crew.

By creating a wingsail with a naturally deformable spanwise-twisting trailing flap, the rolling moment at high wind speeds can be decreased in a naturally occurring, adaptive manner without a substantial penalty in lift and drag. Adaptive wingsails also have an advantage in their dynamic response to sudden changes in wind speed, or gusts. The spanwise flexibility will adaptively reduce the lift on the wing during a sudden increase in wind strength. This reduction in lift will be most

pronounced at the wing tip, providing a limitation on the rolling moment.

In this analysis, the behavior of a wingsail consisting of a rigid airfoil with a flexible flap attached to its trailing edge through a torsion fitting is considered. The individual airfoils of the flexible flap are taken to be rigid in cross- section but deformable in twist in the spanwise direction. The total resistance to spanwise twist deformation of the flap in response to applied aerodynamic moments is characterized by the torsional stiffness, whether this comes from an structural attachment that functions as a torsion rod and/or from the stiffness of the flap airfoil sections to spanwise twist.

In order to focus on the effects of spanwise flexibility on spanwise lift and moment distribution, the spanwise lift distribution will be obtained using strip theory, i.e. local two-dimensional aerodynamic theory. This will provide a good physical understanding of the effects of flap deflection for a high aspect ratio wing without the complexity of three-dimensional analysis. The next step in the analysis would be to apply lifting-line theory to determine the effects of the vortex wake caused by the non-uniform spanwise load distribution, a step that is not taken here.

The analysis first considers a wing of constant chord, which can be solved analytically for this model, then a wing of varying chord, both wings having a flap attached with constant torsional stiffness. Finally a wing of varying chord with a flap of varying torsional stiffness along the span is considered. The non-dimensional parameters necessary to apply these ideas to a wingsail of any size operating in a specified range of wind speeds are also identified.

This analysis also has application to the use of wingsails to power cargo ships. Automatic reduction of rolling moment at high wind speeds due to spanwise flexibility would be especially important for a ship that operates on the open ocean, reducing the work load on the crew while maintaining good safety margins. The analysis is also applicable to extreme sailing competitions, such as round-the-world races, which can encounter extremely dangerous conditions off-shore.

ANALYSIS

Consider a wing of span Y and chord c(y). The wing consists of a rigid airfoil section with a flap attached to the fixed airfoil by a torsion rod of strength κ. The chord of the wing is $c(y)$; for our calculations, we will consider a flap chord that is one half of the local wing chord

$$c_F(y) = 1/2c(y). \tag{1}$$

Initially, the torsional stiffness κ is taken to be constant along the span but clearly its variation could be easily included, as is done in the final case studied.

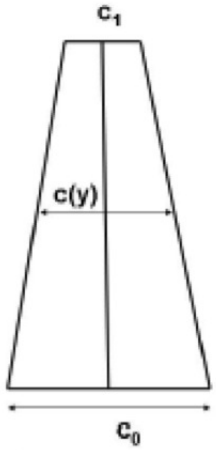

Figure 1 Wing Planform

The wing planform is shown in Figure 1. The front portion of the wing is rigidly supported and held at a constant angle of attack α ; the angle of attack of the flap relative to the wing is $\alpha_1(y)$. Since the interest is in the effect of spanwise flexibility, α_1 is a function of y, determined by aerodynamic loads and torsional stiffness. (For this problem, $\alpha_1(y)$ will be found to be negative; the flap deflection decreases with increasing span.) The airfoil cross-section is shown in Figure 2.

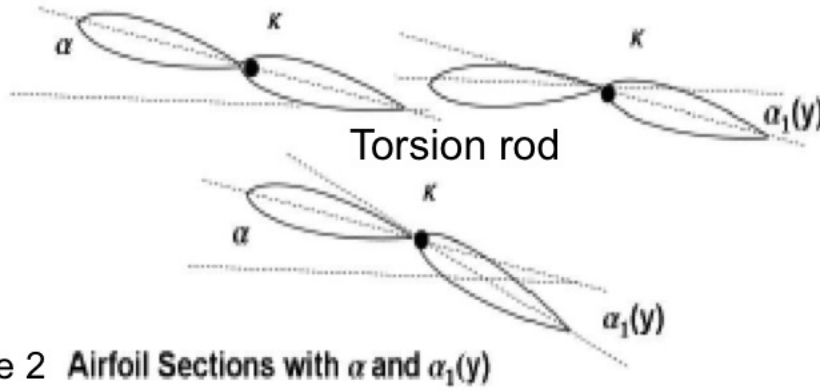

Figure 2 Airfoil Sections with α and $\alpha_1(y)$

To focus on the interaction between aerodynamics and torsional stiffness, two-dimensional linear aerodynamic theory –strip theory–will be used to estimate the effects of spanwise flexibility on the

lift and moment distribution along the span. That is, the airfoil flow is assumed to be locally two-dimensional, and the local lift and moment are integrated along to span to obtain the total results for lift and rolling moment and the spanwise change of flap angle due to aerodynamic moments and torsional stiffness.

At each section, the aerodynamic moment about the attachment point depends upon both α and $\alpha_1(y)$.

$$m(y) = 1/2\rho U^2 c(y)^2 (C_{m_0}\alpha + C_{m_1}\alpha_1(y)) \tag{2}$$

where C_{m_0} and C_{m_1}, the local moment slope coefficients, are available from linear two-dimensional theory. They depend upon the magnitude of the flap chord $c_F(y)$ relative to the total airfoil chord $c(y)$. The moment on the flap acts to reduce the flap deflection α_1.

The relation between the aerodynamic moments and the local angle of attack is given by the torsional stiffness equation.

$$\kappa \frac{d\alpha_1}{dy} = M(y) = \int_y^Y m(y)dy \tag{3}$$

where κ is the torsional stiffness: torque (in ft lbs) per radians/ft of twist: $\kappa = M/\frac{d\alpha_1}{dy}$; κ is a local material property of the structure. $M(y)$ is the total moment at y due to the aerodynamic moment distribution along the span. Figure 3 shows the relationship between the aerodynamic moment $m(y)$ and the torsional moment $M(y)$.

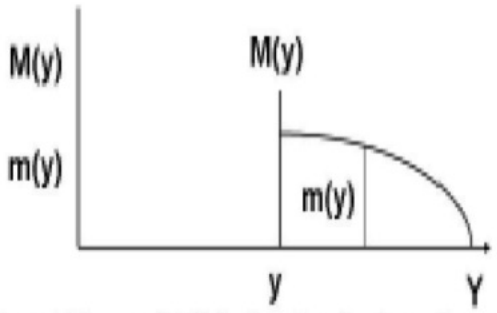

Figure 3 Torsional Moment M(y) at y due to Aerodynamic Moment m(y)

Since the total torsional moment $M(y)$ goes to zero at the tip, the total torsional moment acting at the point y is the integral of the aerodynamic moment $m(y)$ from y to the tip $y = Y$. The governing equation for the unknown flap deflection angle α_1 is given by the derivative of equation (2).

$$\frac{d^2\alpha_1}{dy^2} = m(y) = \frac{\rho U^2 c(y)^2}{2\kappa(y)}(C_{m_0}\alpha + C_{m_1}\alpha_1(y)) \tag{4}$$

This is a linear non-homogenous second order equation for $\alpha_1(y)$. The boundary conditions for the equation are $\alpha_1(0) = \alpha_{1_0}$ and $\frac{d\alpha_1(Y)}{dy} = 0$. That is, the initial flap deflection, α_{1_0}, is set at the root of the wing; and since there is no moment $M(y)$ at the tip, $y = Y$, the slope $\frac{d\alpha_1}{dy}$ is zero at the tip, $y = Y$.

CONSTANT CHORD SOLUTION AND NUMERICAL RESULTS

The governing equation is easily solve if both the chord $c(y)$ is a constant: $c(y) = c_0$, and the torsional stiffness $\kappa(y)$ is a constant, $\kappa(y) = \kappa$. The chord of the flap is taken equal to half of the chord of the total airfoil: $c_F = c_0/2$. The span Y is taken as 4. For this choice, we can easily obtain the various lift and moment distributions along the wing analytically.

The governing equation is characterized by the ratio of the dynamic pressure times the chord c_0^2 divided by the torsional stiffness κ: written for constant chord and constant torsional stiffness we define $Q = \frac{U^2 c_0^2}{2\kappa}$. This results in the governing equation

$$\frac{d^2\alpha_1}{dy^2} - QC_{m_1}\alpha_1 = QC_{m_0}\alpha \tag{5}$$

with boundary conditions $\alpha_1(0) = \alpha_{1_0}$ and $\frac{d\alpha_1(Y)}{dy} = 0$. Defining $A = C_{m_0}Q$ and $B = C_{m_1}Q$ we have

$$\frac{d^2\alpha_1}{dy^2} - B\alpha_1 = A\alpha \tag{6}$$

The solution is

$$\alpha_1(y) = \frac{e^{-\sqrt{B}y}(A\alpha(-1 + e^{\sqrt{B}y})) * (e^{-\sqrt{B}y} - e^{2\sqrt{B}Y}) + \alpha_{1_0}B * (e^{2\sqrt{B}y} + e^{2\sqrt{B}Y})}{B(1 + e^{2\sqrt{B}Y})} \tag{7}$$

From linear airfoil theory for this case, the aerodynamic moments about the flap attachment point due to the deflection of the airfoil α and the deflection of the flap $\alpha_1(y)$, for an airfoil with a flap chord equal to half of the airfoil chord are obtained. These moment coefficients are: $C_{m_0}\alpha = .212\alpha$ and $C_{m_1}\alpha_1(y) = .265\alpha_1(y)$. For later use, the lift coefficients for the airfoil as functions of α and $\alpha_1(y)$ are $C_{L_0} = 2\pi\alpha$ and $C_{L_1} = 5.181\alpha_1(y)$. The torsional stiffness κ is taken as 1.

The results for the total angle of attack of the flap relative to the free stream, $\alpha + \alpha_1(y)$, as a function of y are shown in Figure 4 for a variety of velocities U in fps. The angles α and $\alpha_1(0)$ are taken as 10^o for all wind speeds. The effects of flap spanwise flexibility are clearly seen; $\alpha_1(y)$ goes from its initial value $\alpha_1(0)$ to a negative value at the tip, providing a dramatic reduction in angle of attack at the wing tip. At a wind speed of 60fps, the angle of attack of the flap relative to the free stream flow is dramatically reduced at the tip.

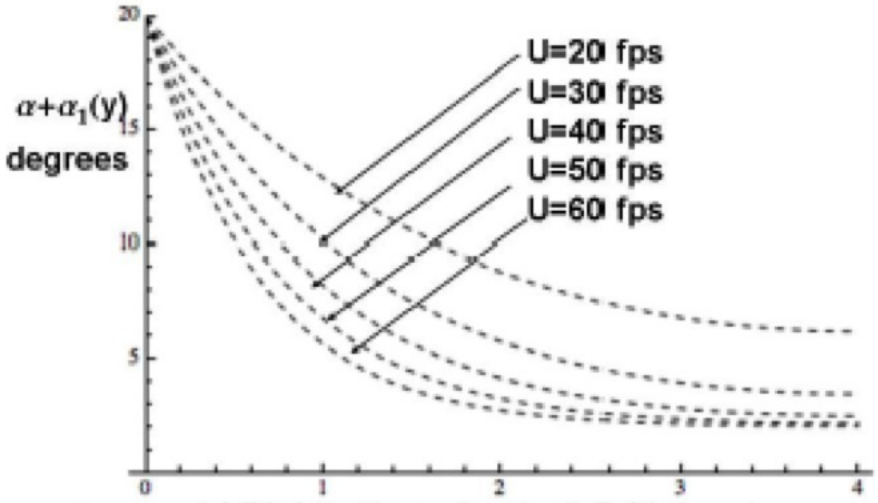

Figure 4 $\alpha+\alpha_1(y)$ Distribution: chord = 1.5; Y=4; κ=1

For a wing of constant chord c_0, the spanwise lift distribution is obtained directly from the angles of attack α and $\alpha_1(y)$, of the wing and the flap, using strip theory.

$$L(y) = 1/2\rho U^2 c_0 C_{L_0} \alpha + 1/2\rho U^2 c_0 C_{L_1} \alpha_1(y) \tag{8}$$

where the lift coefficients C_{L_0} and C_{L_1} have been previously introduced. The spanwise lift distribution is shown In Figure 5 for wind velocities of 20, 30, 40, 50, and 60 fps for a torsional stiffness $\kappa = 1$, $\alpha = 10^o$ and $\alpha_{1_0} = 10^o$. The spanwise lift distribution for a rigid wing at 60 fps is also shown. The reduction of spanwise lift distribution with increasing wind speed due to spanwise flexibility is dramatic.

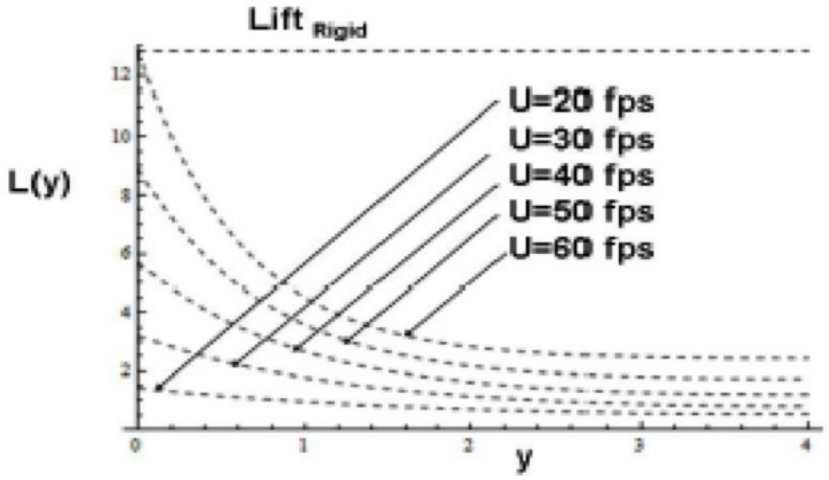

Figure 5 **Spanwise Lift Distribution; Constant Chord**

Figure 6 shows the spanwise lift distribution at a given wind velocity divided by the lift on a rigid wing of the same chord, planform, angle of attack and wind velocity. The effects of spanwise flexibility are clearly evident in the decreased lift outboard of the wing root relative to that of a rigid wing as the wind velocity increases.

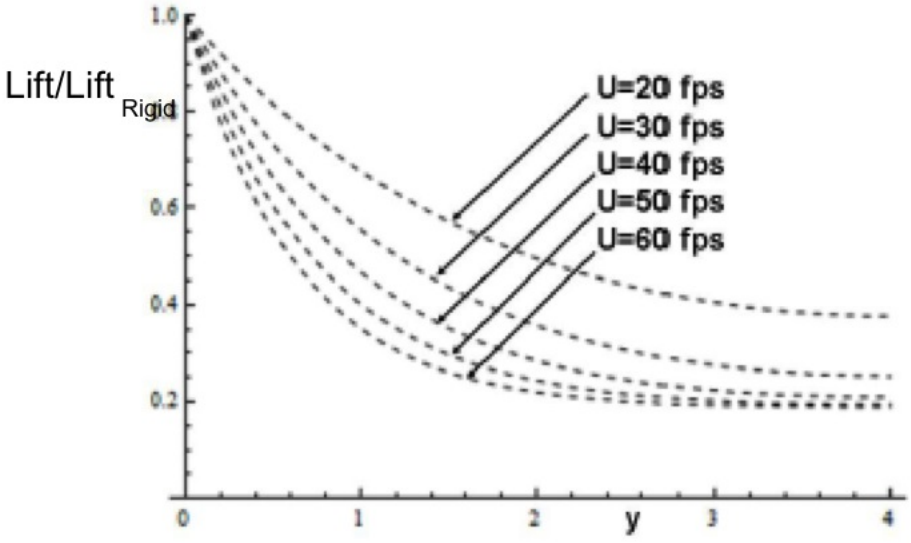

Figure 6 **Spanwise Lift/Lift$_{Rigid}$ Distribution; Constant Chord**

The aerodynamic moment used to characterize the effects of spanwise flap flexibility on wing performance is the moment about the root chord, y = 0: the rolling moment. For a wing of constant chord c_0, the contribution to the rolling moment from each spanwise section y is given by

$$M(y) = 1/2\rho U^2 c_0 (C_{L_0}\alpha + C_{L_1}\alpha_1(y))y \tag{9}$$

For the case examined, the results are shown in Figure 7 for wind velocities of 20, 30, 40, 50, and 60 fps. Also shown is the contribution to the rolling moment from each spanwise section for a rigid wing at a wind speed of 60 fps. The decrease in sectional moment for the flexible flap is clearly evident.

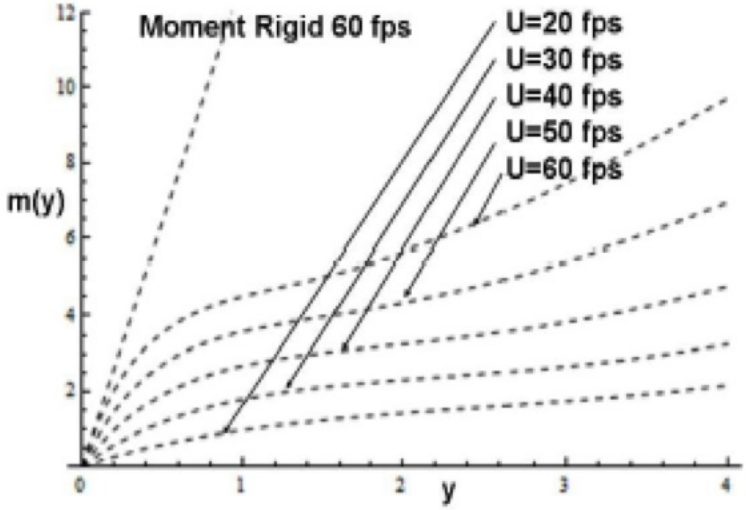

Figure 7 Spanwise Moment Distribution; Constant Chord

The total lift and moment on the wing for a wing of constant chord c_0 is obtained by integrating the sectional lift and moment along the span.

$$L = 1/2\rho U^2 c_0 \int_0^Y ((C_{L_0}\alpha + C_{L_1}\alpha_1(y)dy \tag{10}$$

$$M = 1/2\rho U^2 c_0 \int_0^Y (C_{L_0}\alpha + C_{L_1}\alpha_1(y))ydy \tag{11}$$

Of interest is the ratio of the total lift and total moment on the flexible wing referred to the total lift and moment on a rigid wing of the same planform

$$L_{Rigid} = 1/2\rho U^2 c_0 \int_0^Y (C_{L_0}\alpha + C_{L_1}\alpha_{1_0})dy \tag{12}$$

$$M_{Rigid} = 1/2\rho U^2 c_0 \int_0^Y (C_{L_0}\alpha + C_{L_1}\alpha_{1_0})ydy \tag{13}$$

where α_{1_0} is the initial angle of attack of the flap at the root; for a rigid wing this remains constant along the span. The ratio of lift and moment to that of a rigid wing of the same planform is shown in Figure 8 as a function of velocity U . The difference due to spanwise flexibility is clearly seen, as is the more dramatic effect of flexibility on moment than upon lift.

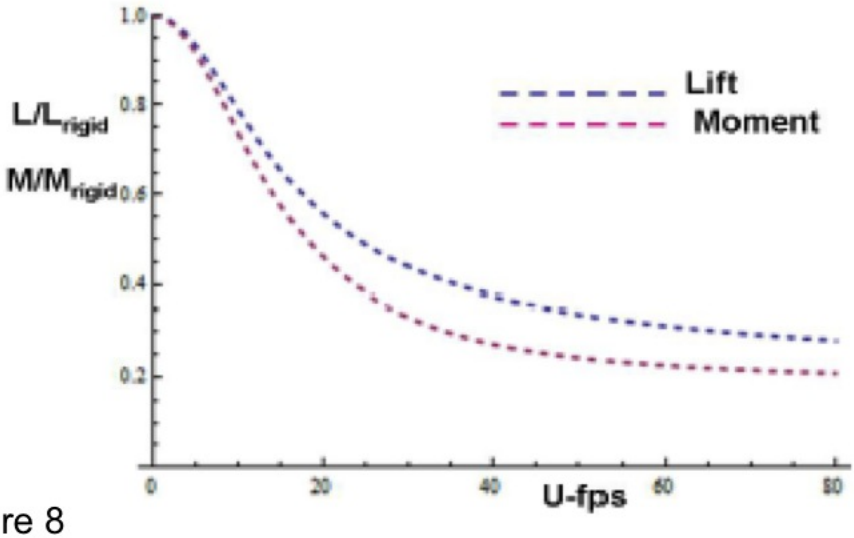

Figure 8
Total Lift and Moment Relative to Rigid Wing vs. U-fps
Constant chord; c_0=1.5; Y=4; κ=1

NUMERICAL SOLUTION FOR A GENERAL WING SHAPE

Now consider a wing of non-constant chord. To compare with the earlier analytic solution, the root chord is taken as $c_0 = 1.5$ and the span is taken as $Y = 4$. The chord is taken with a linear variation to a tip chord of $c_1 = .75$. The chord distribution is then

$$c(y) = c_0 - (c_0 - c_1)\frac{y}{Y} \tag{14}$$

The wing planform is shown in Figure 9. κ can also be taken to vary along the span, although for the initial calculations we take $\kappa = 1$.

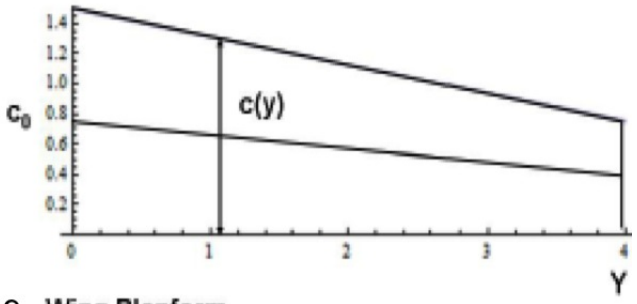

Figure 9 **Wing Planform**

The governing equation remains

$$\frac{d^2\alpha_1}{dy^2} = m(y) = \frac{U^2 c(y)^2}{2\kappa(y)}(C_{m_0}\alpha + C_{m_1}\alpha_1(y)) = A(y)\alpha + B(y)\alpha_1(y) \tag{15}$$

with the inclusion of a chord $c(y)$ that varies with y. The coefficients $A(y)$ and $B(y)$ are as defined in equation (4) and (5), now varying with y: $Q(y) = \frac{\rho U^2 c(y)^2}{2\kappa(y)}$; $A(y) = C_{m_0}Q(y)$; $B(y) = C_{m_1}Q(y)$.

The boundary conditions remains $\alpha_1(0) = \alpha_{1_0}$ and $d\alpha_1/dy = 0$ at y = Y = 4. For this case, κ is again taken as constant: $\kappa = 1$.

The equation is solved numerically for $\alpha_1(y)$ for different values of U : U = 20, 30, 40, 50, and 60 fps. The angle of attack of the wing α is taken as 10^o; the initial angle of attack of the flap $\alpha_1(0)$ is also taken as $\alpha_1(0) = 10^o$.

The results in Figure 10 show the spanwise variation of the total angle $\alpha + \alpha_1(y)$ as a function of wind speed U. The decrease in angle of attack towards the tip due to spanwise flexibility at higher wing speeds is evident.

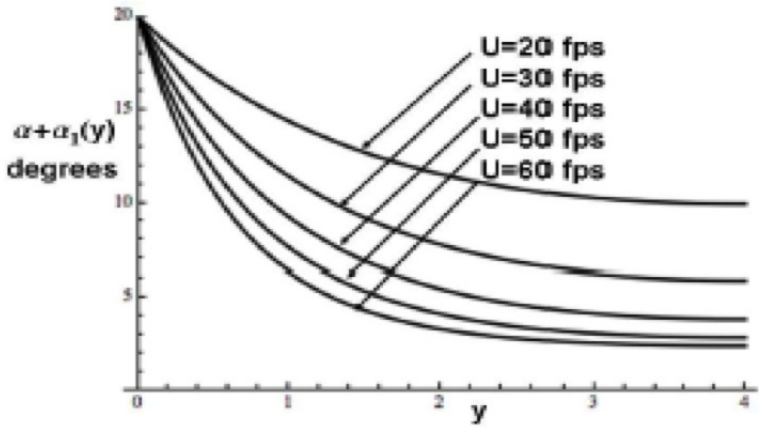

Figure 10 $\alpha+\alpha_1(y)$ Distribution: Y=4; κ=1

Also shown in Figure 11 is a comparison of the constant chord case (dashed) with the varying chord numerical solution. The constant chord solution for local angle of attack is somewhat more affected by spanwise flexibility at lower wind speeds but the overall results are quite similar.

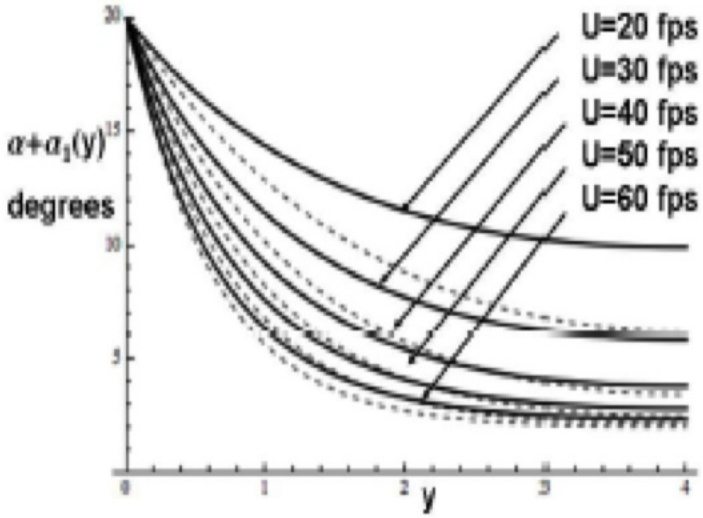

Figure 11 $\alpha + \alpha_1(y)$ Distribution: Y=4; κ=1; Comparison with Constant Chord

The spanwise lift and moment distribution is obtained from the strip-theory formula using the solution for the flexible spanwise distortion of the flap $\alpha_1(y)$. For this case both α and $\alpha_1(0)$ were

taken as 10^o.

$$L(y) = 1/2\rho U^2 c(y)(C_{L_0}\alpha + C_{L_1}\alpha_1(y)) \tag{16}$$

$$M(y) = 1/2\rho U^2 c(y) y(C_{L_0}\alpha + C_{L_1}\alpha_1(y)) \tag{17}$$

Figure 12 shows the spanwise lift distribution L(y) for a variety of wind speeds at constant angle of attack. The effect of spanwise flexibility at higher wind speeds is evident.

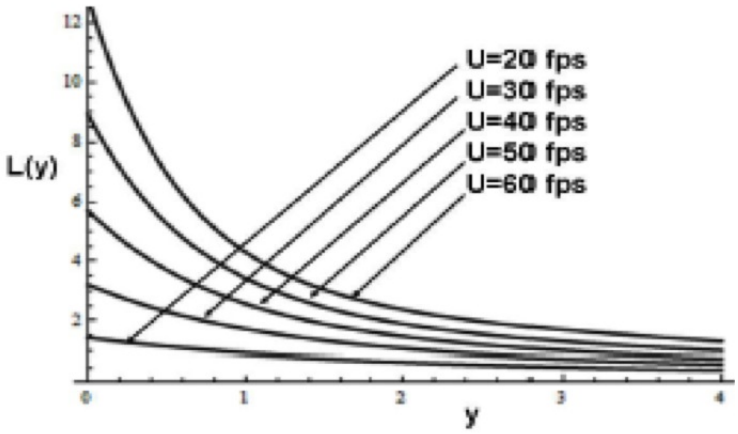

Figure 12 **Spanwise Lift Distribution**

Figure 13 shows the spanwise lift referenced to the lift of a rigid wing of the same geometry. Also shown dashed is the solution for the wing of constant chord at the same root chord and span. The results are quite close especially at higher wind speeds.

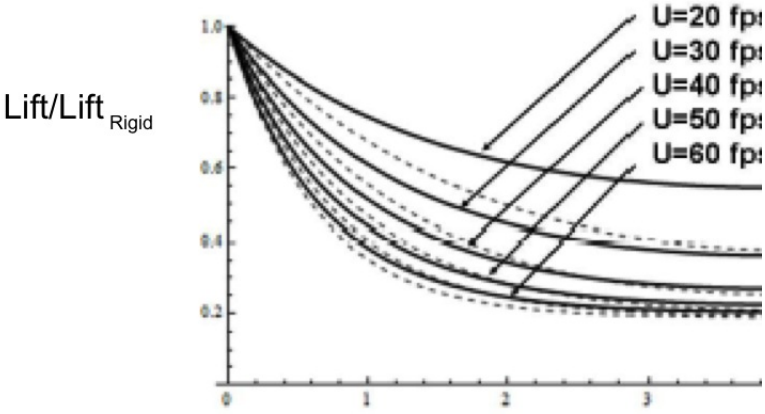

Figure 13 **Spanwise Lift/Lift$_{Rigid}$ Distribution; Comparison with Constant Chord**

Figure 14 shows the contribution to the rolling moment from the various spanwise sections. The spanwise flexibility of the flap acts to decrease the contribution from the outboard sections.

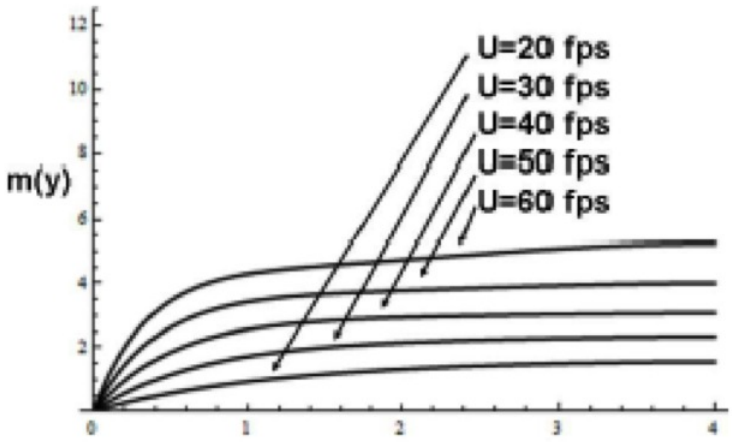

Figure 14 **Spanwise Moment Distribution**

Figure 15 shows the total lift and rolling moment as a function of wind speed, referred to their values for rigid wing of the same geometry. As can be seen, spanwise flexibility greatly reduces the lift and rolling moment at higher wind speeds. The reduction is greater for the rolling moment than for the lift.

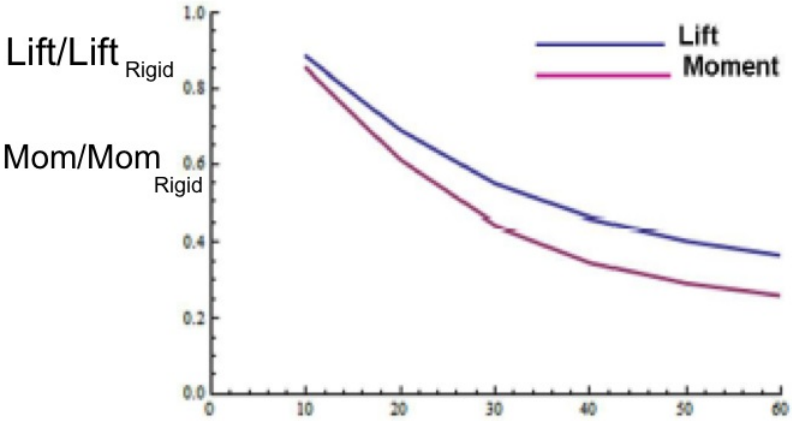

Figure 15 **Lift/Lift$_{Rigid}$ and Moment/Moment$_{Rigid}$ vs.U fps**

Finally, the results for total lift and rolling moment are shown in Figure 16 for both the wing of

constant chord (dashed) and the wing of linearly varying chord (solid), for the same value of root chord $c_0 = 1.5$ and torsional stiffness $\kappa = 1$. The results are very similar, giving the designer a tool for designing a wing for a particular application, for example to maintain a reasonable lift while reducing rolling moment at higher wind speeds in comparison to a rigid wing.

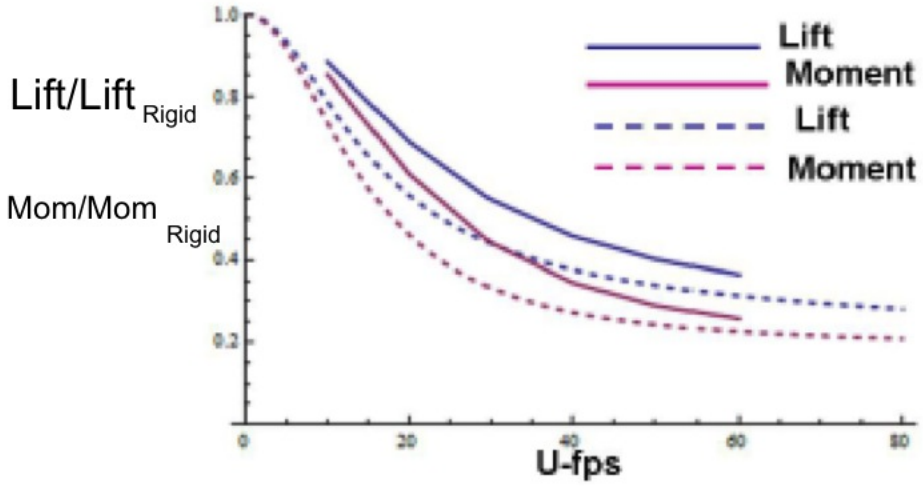

Figure 16 **Lift/Lift$_{Rigid}$ and Moment/Moment$_{Rigid}$ vs. U fps; Comparison with Constant Chord**

In the actual application of these results, the angle of attack would be reduced as the wind speed increases to maintain the constraint on rolling moment. Since the governing equations are linear, the lift and moment scale with the actual value of the angle of attack.

As an example, assume that the constraint on rolling moment is reached at a wind speed of 20fps. Then determine the ratio of lift to rolling moment above 20fps relative to their values at 20 fps using results from this case. As can be seen in Figure 17, if the rolling moment remains constant due to changes in angle of attack, the lift continues to increase, allowing additional thrust to be generated while maintaining constant rolling moment.

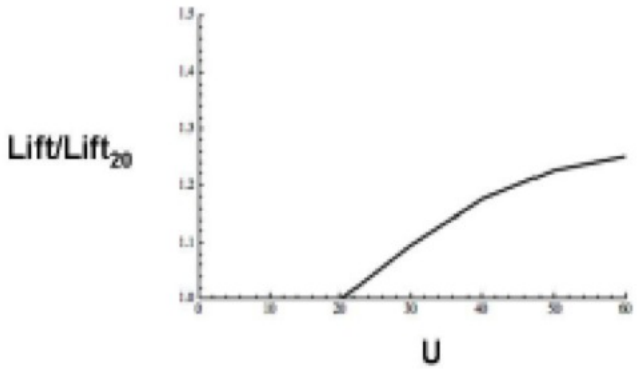

Figure 17 Lift/Lift$_{20}$ vs. U above U$_{crit}$ at Constant Rolling Moment

EFFECT OF SPANWISE VARYING TORSIONAL STIFFNESS

The previous analysis assumed constant torsional stiffness κ along the span. Since the loading at the tip is important for the relief of rolling moment at high wind velocities, it makes sense to examine the effect of varying torsional stiffness $\kappa(y)$ along the span. Assume a linear distribution of $\kappa(y)$ as shown in Figure 18, with $\kappa(0) = 1$; the chordwise variation of chord c(y) along the span is also shown. The torsional stiffness is allowed to decrease dramatically with spanwise distance but is not set to zero at the tip to avoid a singularity in the governing equations. The variation of the coefficients $A(y)$ and $B(y)$ which appear in the governing equations is shown in Figure 19. Strong variation at the tip is again observed.

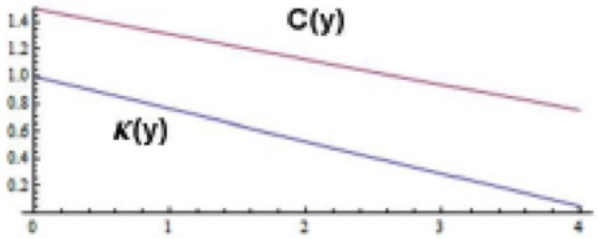

Figure 18 Spanwise Chord and Torsional Stiffness Distribution

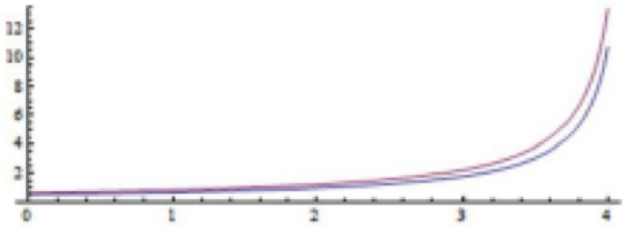

Figure 19 A(y) and B(y) for varying Torsional Stiffness

For this case, the variation of $\alpha_1(y)$ along the span at various wind speeds obtained in the calculations is shown in Figure 20 in comparison with the constant chord, constant torsional stiffness solution. As is expected, there is more variation at the wing tip due to the increased tip flexibility primarily at lower wind speeds.

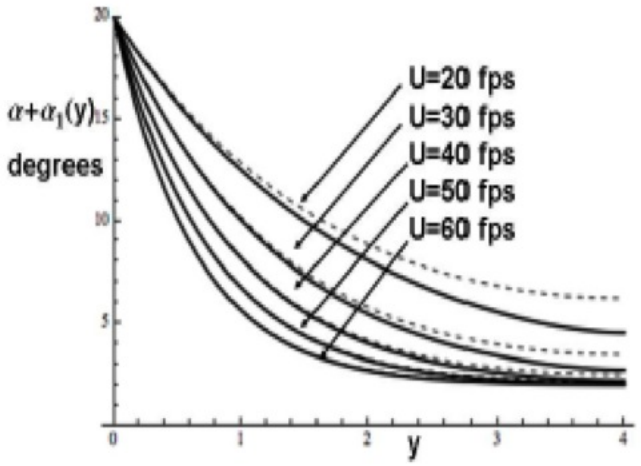

Figure 20 $\alpha+\alpha_1(y)$ vs. y for Different Wind Speeds; Nonuniform Stiffness Comparison with Constant Chord Solution

Shown in the Figure 21 is the spanwise lift distribution at constant angle of attack in comparison with the constant chord, constant torsional stiffness solution. As expected, the lift is reduced at the wing tip at higher wind speeds. Also shown is the spawns lift distribution of a rigid wing at a wind speed of 60 fps.

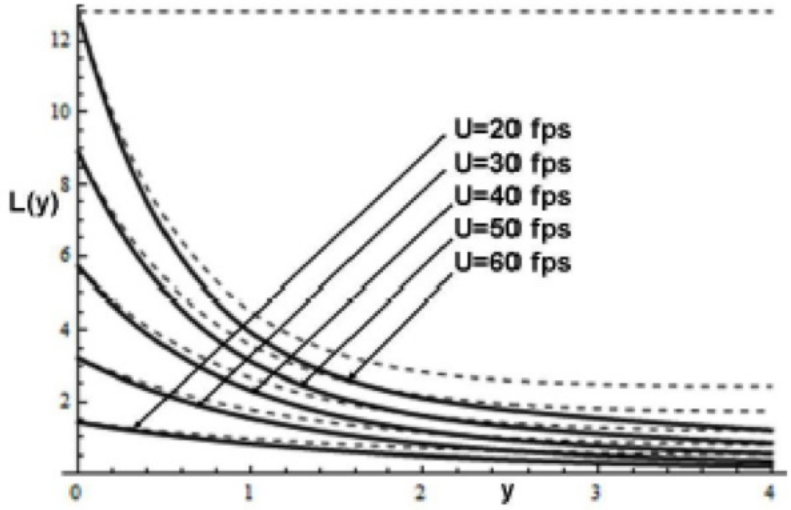

Figure 21 **Spanwise Lift Distribution at Different Wind Speeds; Nonuniform Stiffness; Comparison with Constant Chord Solution**

The spanwise distribution of moment at constant angle of attack is shown in Figure 22. The effect of spanwise flexibility acts to reduce the rolling moment contribution well below that for a rigid wing.

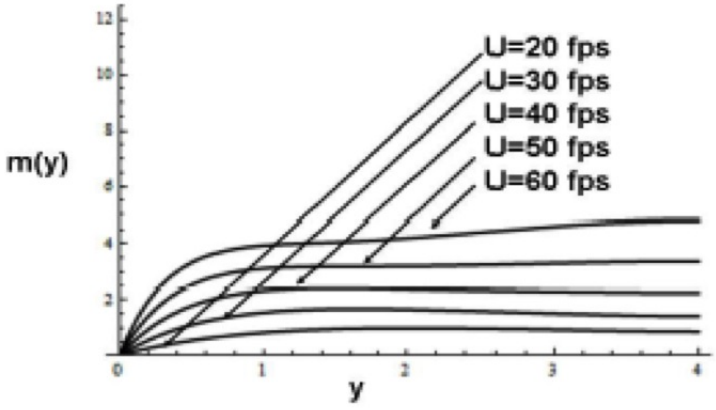

Figure 22 **Spanwise Contribution to Rolling Moment**

These results are shown in Figure 23 in comparison to the constant chord, constant stiffness solution. The decrease in spanwise contribution to the total rolling moment is evident.

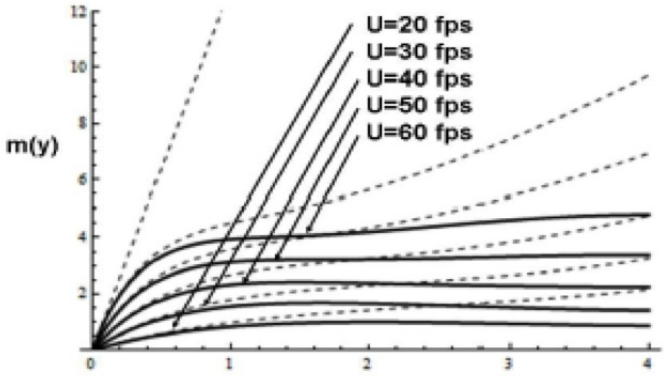

Figure 23 **Spanwise Contribution to Rolling Moment; Comparison to Constant Chord Solution**

Figure 24 below shows the rolling moment relative to its value for a rigid wing as a function of wind speed. Shown is the solution for varying chord and varying torsional stiffness, as well as the solution for constant chord.

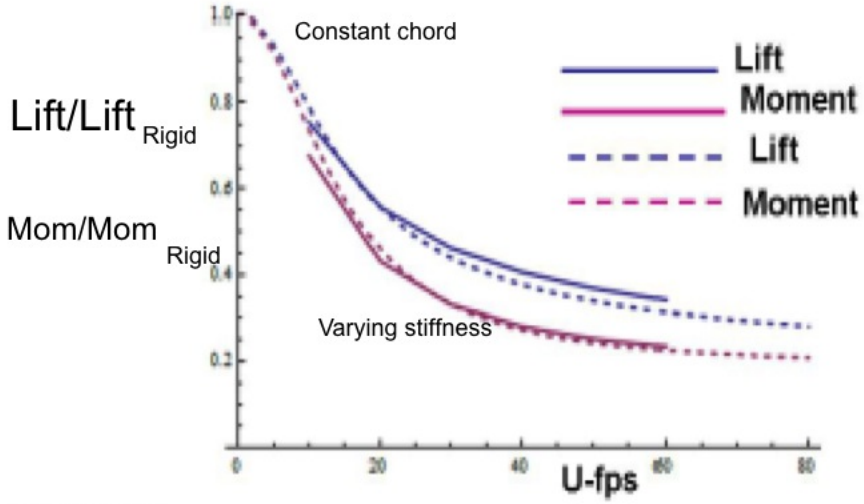

Figure 24 **Total Lift and Moment Relative to Rigid Wing vs. U-fps: Varying Stiffness; Comparison to Constant chord**

Figure 25 compares the results of total lift and rolling moment, relative to that for a rigid wing, for the three cases studied as a function of wind speed. These results give the designer choices to achieve a desired outcome.

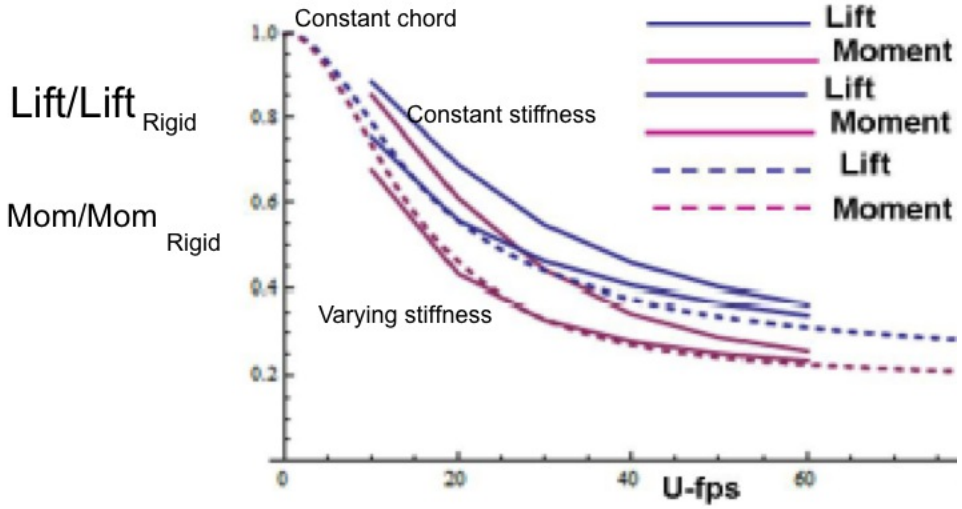

Figure 25 **Total Lift and Moment Relative to Rigid Wing vs. U-f Varying Stiffness; Comparison to Constant Stiffnes Comparison to Constant chord**

NON-DIMENSIONAL ANALYSIS

The previous analysis was conducted for a wing of a specific size, as would be appropriate to predict the outcome of a wind tunnel test. It is straightforward to extend the analysis, using non-dimensional variables, so that the result are applicable to a wing of any size. The requirements on the wing would specify chord c_0, span Y, operating wind speed U and desired behavior. The parameter to be identified for application to a specific wing is the torsional stiffness κ: torque M required in ft lbs per to produce a twist $d\alpha/dy$ in radians/ft. We consider the case of constant chord c_0 for analytic simplicity; the more general case can easily be considered. We begin our analysis with equation (4).

$$\frac{d^2\alpha_1}{dy^2} = m(y) = \frac{\rho U^2 c_0^2}{2\kappa}(C_{m_0}\alpha + C_{m_1}\alpha_1(y)) \tag{18}$$

This equation is written for a wing span from y = 0 to y = Y where Y is the wing span. We non-dimensionalize the equation using the variable $y' = y/Y$. The equation becomes

$$\frac{d^2\alpha_1}{dy'^2} = \frac{\rho U^2 c_0^2 Y^2}{2\kappa}(C_{m_0}\alpha + C_{m_1}\alpha_1(y')) \tag{19}$$

This allows us to identify the governing non-dimensional parameter which we call $\bar{U}$.

$$\bar{U} = \sqrt{\frac{\rho U^2 c_0^2 Y^2}{2\kappa}} \tag{20}$$

We rewrite the equation as

$$\frac{d^2\alpha}{dy'^2} = \bar{U}^2(C_{m_0}\alpha + C_{m_1}\alpha_1(y')) \tag{21}$$

The equation now contains one non-dimensional variable $\bar{U}$ and the two moment coefficients that have already been introduced. The solution follows as before.

We construct the solution for the flap angle $\alpha_1(y')$ for constant chord, since this results in a simple analytic solution.

$$\alpha_1(y') = \frac{e^{-\sqrt{C_{m_1}}\bar{U}y'} * (-\alpha C_{M_0}(e^{2\sqrt{C_{m_1}}\bar{U}} - e^{\sqrt{C_{m_1}}\bar{U}y'})(-1 + e^{\sqrt{C_{m_1}}\bar{U}y'}) + \alpha_{1_0}C_{m_1}(e^{2\sqrt{C_{m_1}}\bar{U}} + e^{2\sqrt{C_{m_1}}\bar{U}y'}))}{C_{m_1}(1 + e^{2\sqrt{C_{m_1}}\bar{U}})} \tag{22}$$

This equation determines $\alpha_1(y')$ for various values of the non-dimensional parameter $\bar{U}$. The results for the total angle of attack $\alpha + \alpha_1(y')$ for $\alpha = 10^o$ and $\alpha_{1_0} = 10^0$. are shown in Figure 26. The reduction in angle of attack due to spanwise flexibility is quite pronounced in the range $8 < \bar{U}$.

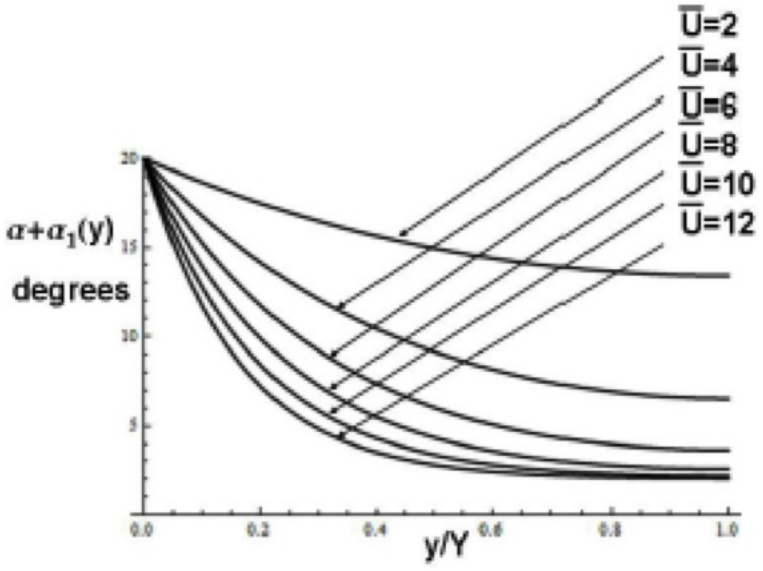

Figure 26 **Spanwise Distribution of Angle of Attack in Degrees as a Function of Non-Dimensionall Velocity**

The spanwise distribution of lift coefficient $C_L(y')$ is in Figure 27 for a range of $\bar{U}$ from 4 to 16 for $\alpha = 10^o$ and $\alpha_{1_0} = 10^0$. The range $8 < \bar{U}$ shows a dramatic decrease in spanwise lift coefficient due to spanwise flexibility.

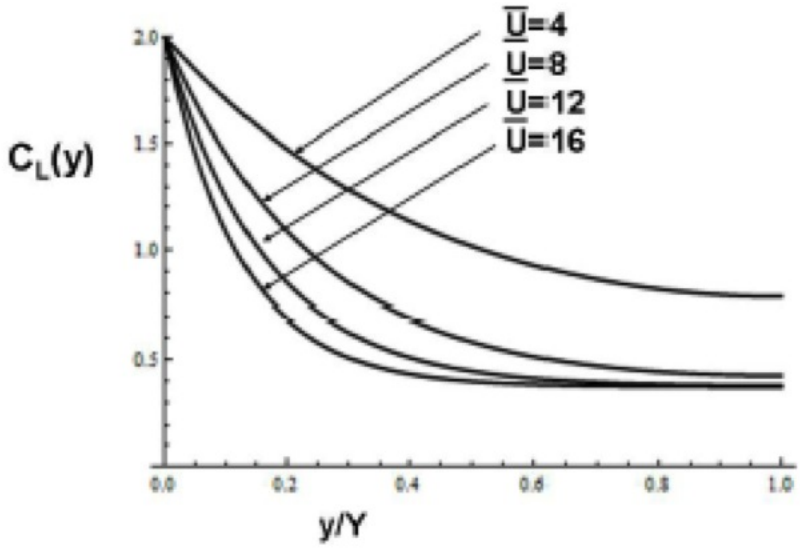

Figure 27 **Spanwise Distribution of Lift Coefficient as a Function of Non-Dimensional Velocity**

The spanwise distribution of rolling moment coefficient $C_M(y_l)$ is shown in Figure 28 for a range of $\bar{U}$ from 4 to 16. The range $8 < \bar{U}$ shows a dramatic decrease in the contribution of outboard wing sections to the rolling moment coefficient due to spanwise flexibility.

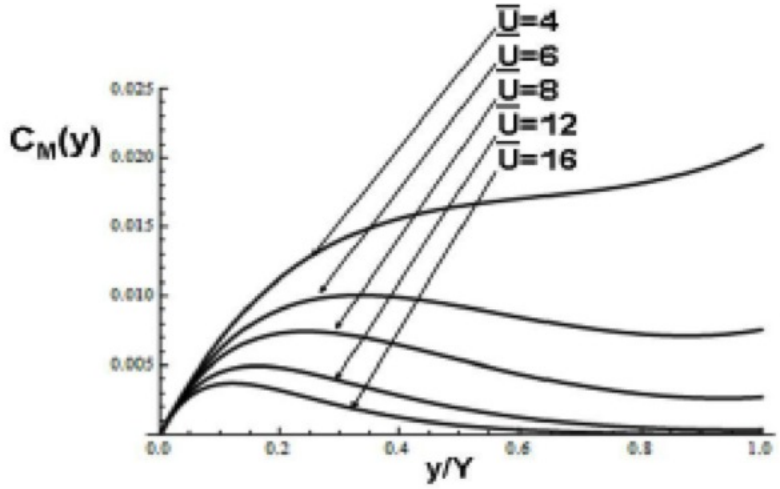

Figure 28 **Spanwise Distribution of Moment Coefficient as a Function of Non-Dimensional Velocity**

We now consider how these non-dimensional results relate to our earlier calculations for a specific

planform. We consider the constant chord solution: Y = 4; $c_0 = 1.5$; and $\kappa = 1$ and $U = 40fps$. This results in a non-dimensionalized $\bar{U} = 8.27$. ($\sqrt{\rho(40)^2 4^2 1.5^2/(2\kappa)} = \bar{U} = 8.27$) We then inquire as to what value of κ would be required to realize this same result (the distribution of $\alpha + \alpha_1(y')$) for a wing of span 70 ft., with a chord of 10 ft. at a wind speed of 25kts. For this case, we set $\sqrt{\rho(25/.59)^2 70^2 10^2/(2\kappa)} = \bar{U} = 8.27$ and obtain the required $\kappa = 15288$. (The factor .59 is the conversion from kts to fps.) Once the spanwise deflection of the flap $\alpha_1(y)$ is determined for a given wind speed, the aerodynamic properties of lift and moment along the span as well as the total lift and total rolling moment can be determined. As previously noted, at higher wind speeds the angle of attack can be reduced to constrain rolling moment while the lift continues to increase, increasing thrust,

REFERENCES

(2013) Fisher, Adam, The Boat That Could Sink the Americas Cup, Wired, May 9, 2013.http://www.wired.com.

(2009) Harmon, Robyn Lynn, Aerodynamic Modeling of a Flapping Membrane Wing Using Motion Tracking Experiments, ProQuest LLC, Ann Arbor, MI, 2009

(1950) Jones, R.T. The Spanwise Distribution of Lift for Minimum Induced Drag of Wings Having a Given Lift and a Given Bending Moment NACA TN2249, 1950

(2010) Junge, Timm, Gerhardt, Frederik C., Richards, Peter, Flay, Richard G.J., Optimizion Spanwise Lift Distributions Yacht Sails Using Extended Lifting Line Analysis, Journal of Aircraft, Vol. 47, No. 6, November-December 2010.

(1997) Sneyd, A.D., Sugimoto, T., The influence of a yachts heeling stability on optimum sail design, Fluid Dynamics Research, Vol. 19,1997,pp.47-63.

(1978) Wood, C.J., Tan, S.H., Towards an optimum yacht sail. Journal of Fluid Dynamics, Vol. 85, Part 3, 1978, pp. 459-477.